Placenta 85 (2019) 24–31

Contents lists available at ScienceDirect

Placenta

journal homepage: www.elsevier.com/locate/placenta

The volume of villi with γ-sm-actin positive perivascular cells correlates with placental weight and thickness

A. Buehlmeyer[a,1], N. Barapatre[a,1], C. Schmitz[a], F. Edler von Koch[b], E. Haeussner[a], H.-G. Frank[a,*]

[a] LMU Munich, Faculty of Medicine, Department of Anatomy II, Pettenkoferstr. 11, 80336, Munich, Germany
[b] Clinic for Obstetrics and Gynecology Dritter Orden, Menzinger Str. 44, 80638, Munich, Germany

ARTICLE INFO

Keywords:
Placenta
Stereology
Volume estimates
γ-sm-actin immunohistochemistry
Villous classification
myofibroblasts
perivascular contractile sheath
contractile villi
non-contractile villi

ABSTRACT

Introduction: The classification of histologically stained villous cross sections in villous types (terminal, intermediate and stem villi) by stromal peculiarities is known to be observer predicated. Therefore, quantitative histology of villous trees has not become a routine endpoint of studies on the role of the placenta in prenatal programming, as opposed to the gross placental parameters weight and thickness. The classification of villous cross sections in central (stem) and peripheral (terminal) parts based on the presence or absence, respectively, of immunohistochemical detection of myofibroblasts in perivascular position is less observer dependent. We hypothesized that it will, possibly, identify microscopic correlates of placental weight and thickness within the villous tree.

Methods: 50 placentas from clinically normal pregnancies were processed for the present study. Thin villous cross sections, obtained in a systematic random manner, were stained immunohistochemically to detect γ-smooth muscle (sm) actin and to classify them subsequently as part of central or peripheral villous tree. The volume fractions of histological structures visible in villous cross sections (stroma, lumen, endothelium and syncytium) were estimated by design-based stereology.

Results: The present study reveals a significant correlation of placental weight and thickness with the volume estimate of stroma that have myofibroblasts in perivascular position.

Discussion: The positive linear correlation between the volume of central parts of villous trees and the placental weight and thickness is new. Surprisingly, the volume of more peripheral parts of villous trees, which is the main site of materno-fetal exchange does not correlate with placental weight and thickness.

1. Introduction

Placental weight and thickness are routine epidemiological parameters in studies of prenatal programming [1,2]. So far, it is unclear, which quantitative histological/microstructural properties of the villous trees correlate with these macroscopic measures of placental size [1,2]. How the volumes of various villous types are associated with the weight of the placenta is one of the basic questions which remains to be investigated.

The classification of villi in stem, intermediate (mature/immature) and terminal villi, based on the microscopic assessment of villous cross sections and as proposed by Kaufmann et al. [3], has been widely used. It has been shown in uncomplicated pregnancies that during gestation the volumetric growth of placenta is largely due to an increase in the volume of terminal villi, while the volume of stem villi remains unchanged [4].

A recent study, however, showed that the classification of villous types according to Ref. [3] is too subjective for quantitative histology [5]. The scatter due to observer dependent (divergent) stroma assessment and subsequent qualitative association to histological types (terminal, intermediate and stem villi) seemed to be too high for statistically powerful assessment of structural differences [5]. Immunohistochemical labelling of, for instance, cytoskeletal elements as markers of perivascular contractile stroma cells (myofibroblasts) in placental villous cross sections was discussed as a possible way forward to develop statistically more powerful and less subjective approaches [5]. The presence of myofibroblasts in massive multilayer arrangement [6], often named as perivascular sheath, in the more central parts of the villous tree can be specifically detected by their immunoreactivity to smooth muscle (sm) actin namely, α-sm-actin and γ-sm-actin [6–9].

* Corresponding author.
E-mail address: hans-georg.frank@med.uni-muenchen.de (H.-G. Frank).
[1] The authors contributed equally.

https://doi.org/10.1016/j.placenta.2019.08.082
Received 27 March 2019; Received in revised form 30 July 2019; Accepted 12 August 2019

The perivascular sheath itself is a structure which is known for a long time [10], but its functional impact is not fully deciphered yet. Since the perivascular sheath thins progressively towards the peripheral regions of the villous tree, only the perivascular stromal compartment of the most peripheral branches of the villous tree is free of α-sm-actin and γ-sm-actin immunopositive cells [6,9]. The immunohistochemical detection of myofibroblasts by marker molecules like γ-sm-actin, hence, can be used as a less subjective classification of villous cross sections as being sections of more centrally located contractile villi or of more peripherally located non-contractile villi.

The global volumes of various villous types can be estimated by design-based stereology. It is a powerful tool for estimating, among others, constitutive volume fractions of any specimen by merely studying its cross sections with two-dimensional (2D) or three-dimensional (3D) probes. Representative quantitative values can be obtained by design-based approaches with minimal bias [11]. It has been applied successfully in placenta research for quantitative assessment of, for example, mismatches of status of villous growth and gestational age in an economical and efficient manner [12].

Previous quantitative histological studies of the human placental villous tree based on observer predicated stromal classification might have missed relevant correlations with macroscopic placental data like placental weight and thickness. Working on this premise, the present study was undertaken to discriminate between the central and peripheral parts of the villous trees based on the immunohistochemical detection of γ-sm-actin in the cytoskeleton of placental myofibroblasts in the perivascular compartment of the villous stroma. Concurrently, the endothelial marker CD34 was detected to identify the fetal endothelium and to assist in identifying perivascular locations in small caliber villi. The volumes of γ-sm-actin positive and γ-sm-actin negative villous compartments were estimated by design-based stereology for placentas of uncomplicated pregnancies. These volumes were then correlated with placental weight and thickness to reveal a symmetric or asymmetric contribution of these villous subvolumes to differences in placental weight and thickness.

2. Materials and methods

2.1. Origin of study material

This project was approved by the ethics committee of the Ludwig-Maximilians-University (LMU) Munich, Germany, under the number 084-11. Fifty term placentas of clinically normal pregnancies were obtained from women, who had given their informed consent prior to the study. The classification of pregnancy as clinically normal was done by the obstetrician co-author (FEvK). All placentas were collected at the Department of Obstetrics and Gynecology of the hospital Dritter Orden, Munich, Germany. Immediately after delivery, the placentas were stored in a refrigerator between 4 °C and 7 °C. The placentas were subsequently transported to the processing laboratory in cooled and thermally insulated bags.

2.2. Tissue sampling and processing

Before sampling and fixation, the macroscopic parameters of the placentas were measured. The placentas were positioned in a flat tray with the chorionic side facing up. Then the weight, the thickness and the longest and the shortest diameter were measured. Placental thickness was determined ultrasonically by placing the probe (Convex Scanner HS 3000, Honda Electronics, Tokyo, Japan) gently and without pressure on the chorionic surface near the umbilical cord. Later, six sampling sites per placenta were chosen in a systematic random manner by projecting a regularly spaced point pattern onto the chorionic surface of the placenta. Full-depth tissue columns were obtained from these six sites, fixed in 4.5% phosphate buffered formalin for at least 24 h at 4 °C, and finally were embedded in paraffin cuboids with edge lengths of about 2.5 × 1.2 × 1.8 cm. Samples were allowed to drown in liquid paraffin without any optimisation of orientation by manual positioning. One 4 µm thick section was taken from each sample and stained immunohistochemically for stereological analyses.

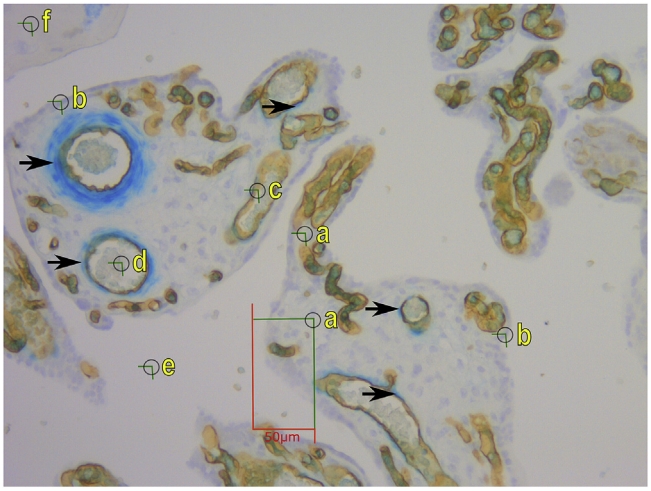

Fig. 1. The figure shows an immunohistochemically stained section with exemplary villous cross sections. It also exemplifies the point counting procedure and allocation of counting points to subvolumes. The counting frame is represented by the rectangle created by red and green lines, whereby the upper right corner of the counting frame (marked by a circle) is treated as the counting point. Letters **a-e** represent possible positions of the counting point on the section. The blue stain shows positive immunoreactivity for γ-sm-actin and is indicated by arrows. The brown stain marks the surface molecule CD34 in vasular endothelium. Two villous cross sections in the central part of the figure show prominently the perivascular reactivity for γ-sm-actin (arrows). Following positions were assigned to the various subvolumes. **(a)** Stroma of a γ-sm-actin positive villous cross section (posSTRO). **(b)** Villous trophoblast of a γ-sm-actin positive villous cross section (posSYN). **(c)** Endothelium of a γ-sm-actin positive villous cross section (posENDO). **(d)** Lumen of a vessel of a γ-sm-actin positive villous cross section (posLUM). **(e)** Intervillous space (IVS). **(f)** Fibrinoid (FIB).

2.3. Immunohistochemistry

Immunohistochemical double staining of the perivascular sheath and the fetal villous endothelium was performed as described in Ref. [13]. Briefly, the sm-actin present in the perivascular myofibroblast-like cells [9] was labeled immunohistochemically using the antibody kit anti-γ-sm-actin (1:900 in PBS buffer; article no. 69133; MP Biomedicals, Eschwege, Germany) with a secondary antibody and labeling with beta-galactosidase to allow for indigo-blue visualization of myofibroblasts with X-Gal (article no. B1690; Invitrogen, Dreieich, Germany) as substrate. The surface molecule CD34 present in the endothelium of fetal vessels inside the villous trees was stained with anti-CD34 (1:900 in PBS buffer; article no. MS-363-PO; Thermo Fisher Scientific, Dreieich, Germany; visualisation with peroxidase as label and DAB-Brown as microscopic marker). The immunohistochemical reactions were performed as per protocols provided with the antibody kits. Nuclei in the sections were counterstained with hematoxylin to support histological orientation during microscopic analysis.

2.4. Stereological Analyses

The point-counting technique developed by Thomson [14] together with a design-based approach, as recently reviewed by Schmitz and Hof [11], was employed to estimate the volume fractions of γ-sm-actin positive and γ-sm-actin negative components of the villous trees from a single thin section of each paraffin block. The stereological analyses were performed with a computerized stereology workstation, which comprised of a modified light microscope (Axioskop, Zeiss, Jena,

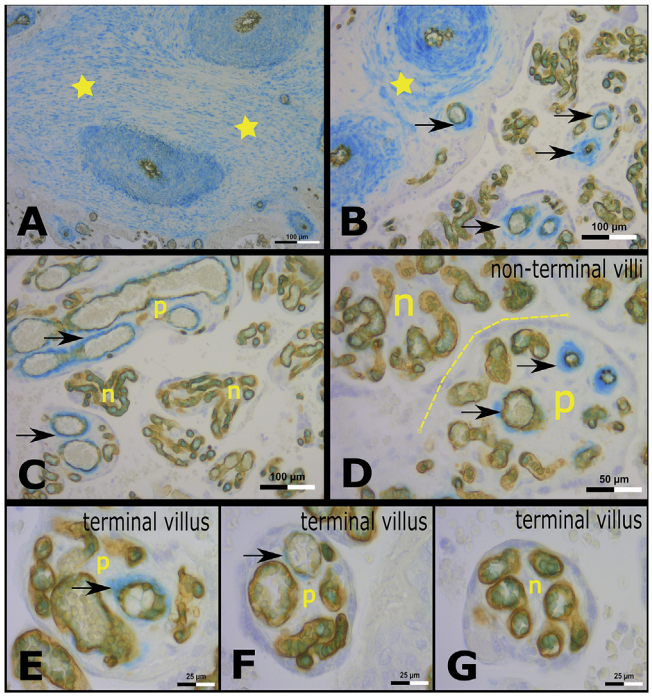

Fig. 2. Tiles **A-G** show villous cross sections and the distribution of immunohistochemical reactivity after detection of CD34 (brown stain, vascular endothelium) and γ-sm-actin (blue stain). **A, B** show cross sections of large (**A**) and intermediate caliber (**B**) stem villi. In perivascular areas outside the brown CD34 labeling and the vascular media, there is γ-sm-actin reactivity (yellow astersisks). Small caliber stem villi show single layer reactivity directly surrounding the CD34 positive endothelium (arrows in **B**). In **C**, neighbouring villous cross sections are labeled as γ-sm-actin positive (yellow p and arrow on blue perivascular γ-sm-actin labelling) and γ-sm-actin negative (yellow n). The γ-sm-actin positive cross sections can be classified histologically as mature intermediate villi or as small stem villi, while the γ-sm-actin negative cross sections can be classified histologically as terminal villi. In **D**, two villous cross sections (separated by a yellow dashed line) with very similar histological properties are discriminated as γ-sm-actin positive (yellow p) or negative (yellow n). Tiles ***E*-G** show cross sections of villi which can histologically all be classified as terminal villi. Strong (**E**) or weak (**F**) reactivity for γ-sm-actin (arrows) renders the cross sections in **E** and **F** as γ-sm-actin positive (yellow p). The cross section in **G** is γ-sm-actin negative (yellow n).

Germany) and a motorized specimen stage for automatic sampling (MBF Bioscience, Williston, Vermont, USA). The driving software was Stereo Investigator (version 11.02; MBF Bioscience, Williston, USA). Using the "Optical Fractionator Workflow" of Stereo Investigator, a contour encompassing the whole section was drawn at 2x magnification. Then, a regular grid containing 300 measurement fields was placed on the section. Each field was viewed at 40x magnification and a counting frame (vertical 100 µm; horizontal 50 µm) was projected over it to enable a variety of stereological procedures. Of these, only the point-counting procedures leading to volume estimates are evaluated in the present study. The top right corner of the counting frame was chosen as the counting point. All points belonged either to intervillous space (IVS), to fibrinoid (FIB) or a villous cross sections, which either showed presence of myofibroblast by indigo-blue perivascular labelling of γ-sm-actin, or its absence. Following histological structures stroma (STRO), vascular lumen (LUM), endothelium (ENDO), syncytiotrophoblast (SYN), and the sum of all these villous subvolumes (SU) were considered part of the villous cross sections they were located on and inherited the property of either being part of a villous cross section staining positive (pos) for perivascular γ-sm-actin (posSTRO, posLUM, posENDO, posSYN and SUpos) or being part of a villous cross section staining negative (neg) for perivascular γ-sm-actin (negSTRO, negLUM, negENDO, negSYN and SUneg). This microscopic procedure is exemplified and explained in Fig. 1. The classification of the histological structures was undertaken by a single observer. Finally, estimates of volume fractions were calculated for each structural component by taking the ratio of points hitting a particular structure (e.g. posSTRO) and total sampled points. These relative volumes were indexed in the variable names (e.g. as $posSTRO_{rel}$). Absolute volumes were estimated by multiplying these volume fractions with the volume of the placenta, which was derived from PW by assuming the tissue density to be 1.05 g/ml [15]. These absolute volumes [ml] were indexed in the variable names (e.g. as $posSTRO_{abs}$).

Table 1
A: Descriptive statistics of clinical macroscopic parameters. The mean and standard deviation (± SD) values are given for the variables gestational age (GA), birth weight (BW), placental weight (PW), the placental weight to birth weight ratio (PW/BW), longest diameter (LD) and the shortest diameter (SD) of the chorionic disk, the surface area (area) of the placental disk, and the placental thickness. **B:** The mean and standard deviation (± SD) values are given for following volumes estimates of microscopic parameters in relative and absolute units. Data are of stroma of γ-sm-actin positive or negative villous cross sections (posSTRO and negSTRO), of vascular lumen of γ-sm-actin positive or negative villous cross sections (posLUM and negLUM), of endothelium of γ-sm-actin positive or negative villous cross sections (posENDO and negENDO), of (syncytio-)trophoblast of γ-sm-actin positive or negative villous cross sections (posSYN and negSYN), of the sum of volume estimates of all γ-sm-actin positive or negative villous parts (SUpos and SUneg), and of the sum of all villous parts (SU), fibrinoid (FIB) and intervillous space (IVS).The data are presented as relative volumes (Volume Fraction [%]) and as absolute volumes (Volume [ml]).

A:	Parameter	Mean	±SD	n
	GA (week)	39.65	±1.20	50
	BW (g)	3410	±426	50
	PW (g)	503	±94	50
	PW/BW ratio	0.149	±0.028	50
	LD (cm)	19.63	±1.82	50
	SD (cm)	16.35	±2.00	50
	Area (cm^2)	1012	±177	50
	Thickness (cm)	1.586	±0.427	50
B:		**Volume Fraction [%]**	**Volume [ml]**	
	Volume Estimates	**Mean ±SD**	**Mean±SD**	**n**
	posSTRO	14.35 ± 28.37 [%]	72.37 ± 20.53 [ml]	50
	posLUM	5.70 ± 47.34 [%]	28.73 ± 13.60 [ml]	50
	posENDO	1.40 ± 52.27 [%]	7.06 ± 3.69 [ml]	50
	posSYN	2.50 ± 41.70 [%]	12.59 ± 5.25 [ml]	50
	SUpos	23.94 ± 7.22 [%]	120.75 ± 36.42 [ml]	50
	negSTRO	6.01 ± 50.26 [%]	30.30 ± 15.23 [ml]	50
	negLUM	5.22 ± 52.00 [%]	26.31 ± 13.68 [ml]	50
	negENDO	1.56 ± 80.90 [%]	7.89 ± 6.38 [ml]	50
	negSYN	2.93 ± 41.52 [%]	14.74 ± 6,12 [ml]	50
	SUneg	15.71 ± 6.76 [%]	79.23 ± 34.09 [ml]	50
	SU	39.66 ± 7.34 [%]	200.00 ± 37.03 [ml]	50
	FIB	9.53 ± 49.25 [%]	48.08 ± 23.68 [ml]	50
	IVS	50.81 ± 23.33 [%]	256.27 ± 59.78 [ml]	50

2.5. Statistical Analysis

The relative and absolute volume estimates of γ-sm-actin positive components (posSTRO, posLUM, posENDO, posSYN and SUpos), γ-sm-actin negative components (negSTRO, negLUM, negENDO, negSYN and SUneg), fibrinoid (FIB) and intervillous space (IVS) were correlated with the macroscopic parameters birth weight (BW), placental weight (PW), placental thickness and the ratio PW/BW. From each of the six sections of each placenta, mean values and standard deviations were calculated to allow for estimation of intraplacental variability. Since intraplacental variability was not different, the aggregated placental means obtained from the six samples of each placenta were used for further analysis. Linear regression analysis (without *p*-value correction) and box plot analysis (Mann-Whitney t-Tests) were performed with

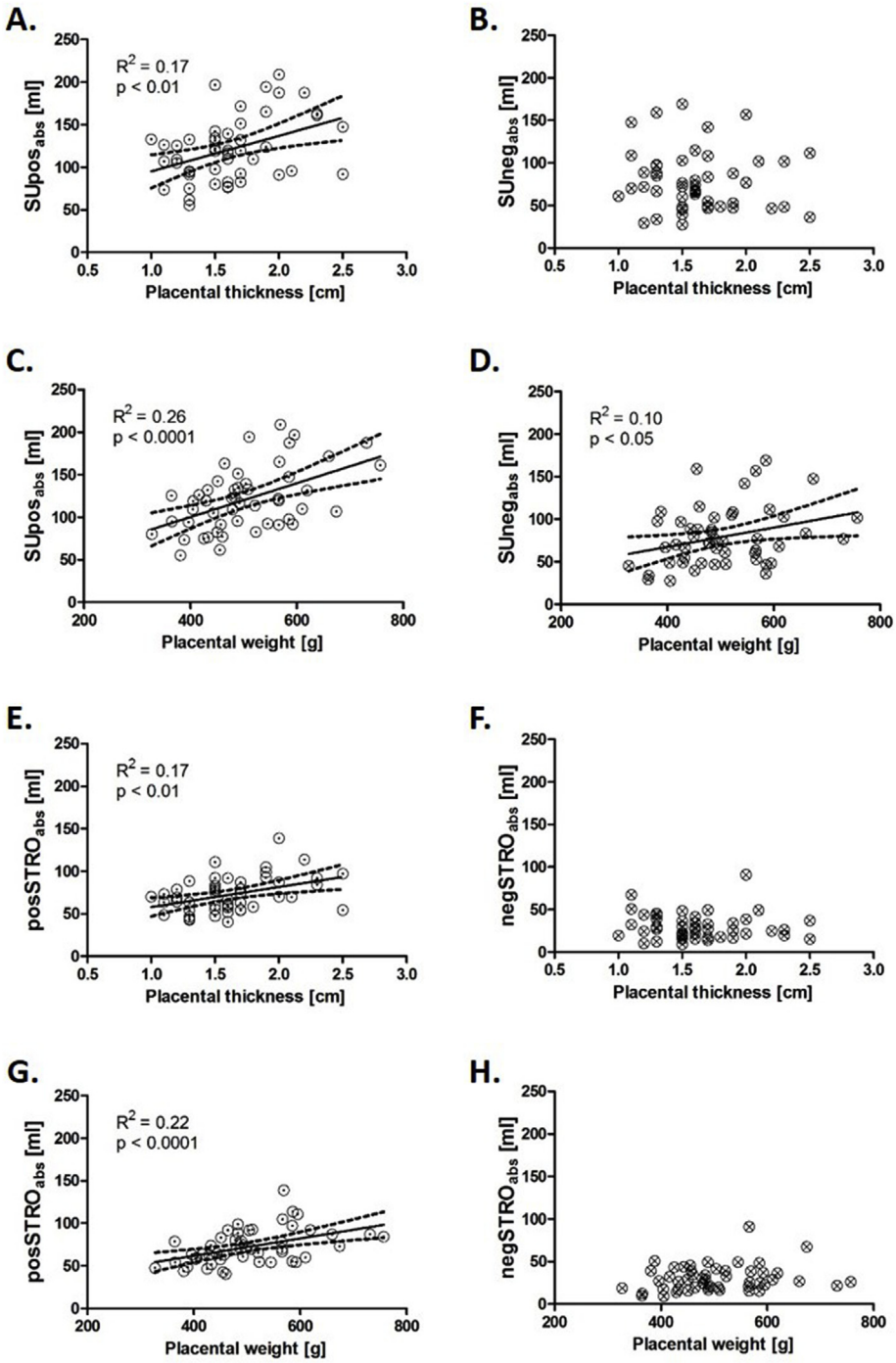

Fig. 3. A.-H. show linear regression analyses without p-value correction. The linear regression line, the 95% confidence interval (dotted lines), R^2 , and the p-value of the linear regression analysis is included in the graphs. For tiles without linear regression line, confidence interval, p-value and R^2, the slope of the regression line was not significantly different from zero. The tiles graph data of absolute volumes [ml] derived from γ-sm-actin positive (dotted circles, **A., C., E., G.**) or from γ-sm-actin negative (crossed circles, **B., D., F., H.**) villous cross sections. **A.-B.** show placental thickness [cm] with SUpos$_{abs}$ [ml] (**A.**), or SUneg$_{abs}$ [ml] (**B.**). **C.-D.** show placental weight [g] with SUpos$_{abs}$ [ml] (**A.**), or SUneg$_{abs}$ [ml] (**B.**). **E.-F.** show placental thickness [cm] with posSTRO$_{abs}$ [ml] (**E.**), or negSTRO$_{abs}$ [ml] (**F.**). **G.-H.** show placental weight [g] with posSTRO$_{abs}$ [ml] (**G.**), or negSTRO$_{abs}$ [ml] (**H.**).

GraphPad Prism (version 5.04; GraphPad, San Diego, USA). The multiparametric correlation analysis with Benjamini-Hochberg correction for *p*-values [16] was done with R software and its packages *psych* and *car* [17–19].

3. Results

3.1. Immunohistochemical discrimination of villous type

The villous cross sections were unambiguously classified as showing γ-sm-actin reactivity in perivascular position or not showing γ-sm-actin reactivity in perivascular position. We observed that this dichotome immunohistochemical allocation of villous cross sections was different from the conventional allocation of villous cross sections to villous types (i.e. stem villi, intermediate villi, and terminal villi). Large stem villi regularly showed abundant, often multilayered γ-sm-actin reactivity in perivascular position (Fig. 2A–C). However, intermediate cross sections of villi (histologically non-terminal villi; Fig. 2D) and small cross sections of villi (histologically terminal villi; Fig. 2E–G) occurred with or without γ-sm-actin reactivity in perivascular position. Principally, γ-sm-actin reactivity in perivascular position occurred in villous cross sections which represent all villous types of the conventional histological classification (i.e. stem villi, intermediate villi, and terminal villi).

The volumes of types of villi, as discriminated immunohistochemically, are listed in Table 1. SUpos$_{abs}$ was larger than SUneg$_{abs}$. Specifically, posSTRO$_{abs}$ was larger than negSTRO$_{abs}$ (Table 1).

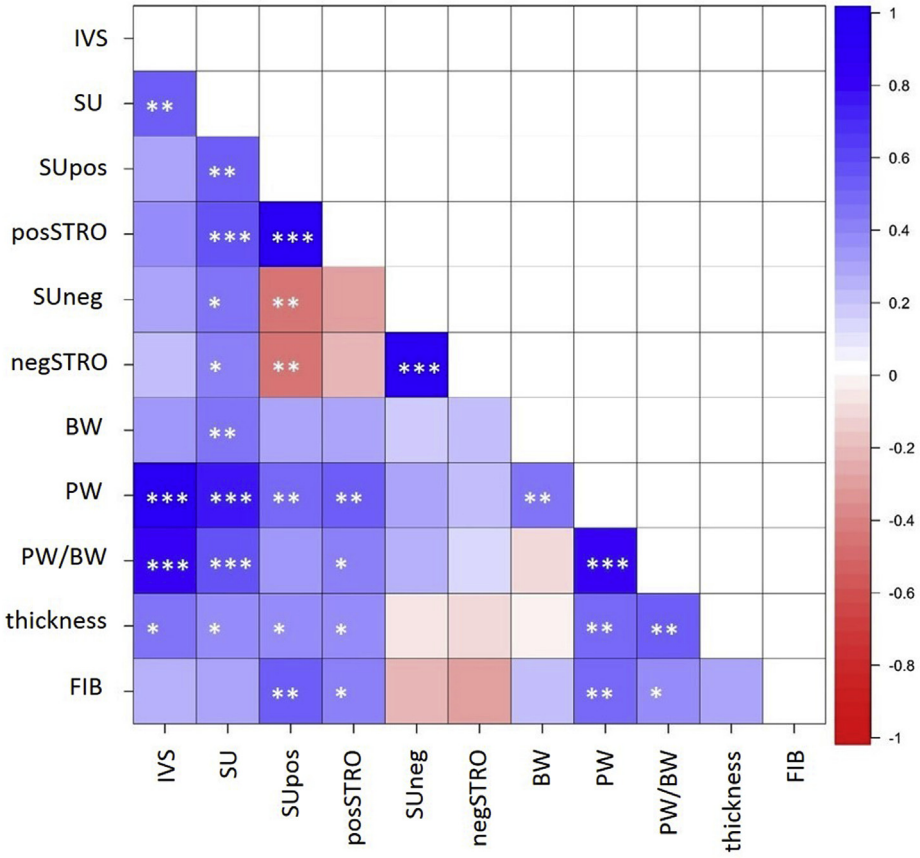

Fig. 4. Result of the multiparametric correlation analysis is graphically depicted by means of a heat map. All parameters IVS_{abs}: volume [ml] of the intervillous space; SU_{abs}: sum of all villous volumes [ml]; $SUpos_{abs}$: sum of volume estimates [ml] derived from all subvolumes of γ-sm-actin positive villous cross sections; $posSTRO_{abs}$: stroma volume derived from γ-sm-actin positive villous cross sections; $SUneg_{abs}$: sum of volume estimates [ml] derived from all subvolumes of γ-sm-actin negative villous cross sections; $negSTRO_{abs}$: stroma volume derived from γ-sm-actin negative villous cross sections; BW: birth weight [g]; PW: placental weight [g]; PW/BW: placental weight to birth weight ratio; thickness: placental thickness [cm]; FIB_{abs}: Volume of fibrinoid [ml]. To avoid data redundancy, only the fields below the matrix diagonal are filled. The p-values are after post-hoc correction for multiple bivariate testing according to Benjamini-Hochberg [16] and are symbolized by asterisks (*) in the comparisons ($p < 0.05$ *; $p < 0.01$ **; $p < 0.001$ ***). Further, the correlation between the variables is color-coded according to the scale bar shown on the right side of the figure. A positive correlation is shown in blue, while red depicts a negative correlation. The shades of both colors get darker with increasing strength of the correlation with +1/-1 being strongest correlations. 0 (white) represents no correlation between the variables.

3.2. Correlational analysis of volume estimates

A simple regressional analysis, without *p*-value correction for multiple comparisons, revealed a statistically significant linear correlation of PW with Thickness and IVS (Fig. ure_S1)Supplementary Fig. 1. An increase in PW was accompanied by an increase in the Thickness and IVS. Similarly, statistically significant linear correlations were observed between $SUpos_{abs}$ and PW and Thickness (Fig. 3 A, C). On the other hand, $SUneg_{abs}$ correlated significantly with PW (Fig. 3 B), but not with Thickness (Fig. 3 D). It means that, while an increase in PW is accompanied by an increase in the sum of volume estimates of both, γ-sm-actin positive and γ-sm-actin negative villous subvolumes, only $SUpos_{abs}$ is dependent on Thickness.

Further, a statistically significant linear correlation was observed between the volume of $posSTRO_{abs}$ and PW and Thickness (Fig. 3 E, G), before the *p*-value correction. No such dependence was observed between volume of $negSTRO_{abs}$ and PW and Thickness (Fig. 3 F, H).

The multiparametric correlation analysis with *p*-value correction for multiple comparisons was adopted to eliminate chance significant results. The results are shown in form of a heat map in Fig. 4. It shows that IVS and SU increase with increasing PW and Thickness. Also, an increase in volumes of $SUpos_{abs}$ and $posSTRO_{abs}$ is observed with increasing PW and Thickenss. On the other hand, $SUneg_{abs}$ and $negSTRO_{abs}$ correlate neither with PW nor with Thickness.

FIB correlates significantly with $SUpos_{abs}$ and $posSTRO_{abs}$, but not with any of the parameters IVS, SU, $SUneg_{abs}$, or $negSTRO_{abs}$ (Fig. 4). In addition, we observed a statistically significant correlation of IVS with the PW/BW ratio (Fig. 4).

Fig. 5 shows the effect of the mode of delivery (vaginal and *sectio caesarea*) on various morphometric parameters evaluated in this study. The ratio PW/BW, IVS and $negLUM_{abs}$ were the only parameters, which were statistically significantly different with regard to the mode of delivery (Fig. 5). All three parameters were significantly higher in the sectio group than the vaginal group.

4. Discussion

Gross morphological parameters such as PW and Thickness are relevant readouts of many perinatal studies (see e.g. Refs. [20–23], especially of studies with a focus on prenatal programming) and point to subclinically different courses of clinically normal pregnancies [21,24] with a lifelong health burden associated to them (see e.g. Refs. [25,26]). So far, the macroscopic findings on weight and thickness could not be translated into microscopic correlates in clinically normal placentas. For the first time, the present study identifies microscopic morphometric parameters which correlate with these macroscopic placental data.

Specifically, the present study shows that $SUpos_{abs}$ and $posSTRO_{abs}$ correlate significantly with PW and Thickness (Fig. 4). The data reveal that with increasing volume of $SUpos_{abs}$ and $posSTRO_{abs}$, PW and Thickness increase, too. This relationship could not be observed with $SUneg_{abs}$ and $negSTRO_{abs}$.

$SUpos_{abs}$ and $posSTRO_{abs}$ are volumes which belong to the more central parts of the villous trees, including the chorionic main stems of the villous system and their first generation branches. This becomes clear from the presence of myofibroblasts in perivascular position which was qualitatively shown in the present study and is in line with current knowledge [6–10]. The data of the present study also show that the volume of fibrinoid (FIB) correlates with $SUpos_{abs}$ and $posSTRO_{abs}$, which is likely reflecting the main site of occurrence of fibrinoid of the villous trees at the surface of the more centrally located stem villi [9,27].

Since the postnatal health profile of newborns after clinically normal pregnancies correlates with placental weight and placental

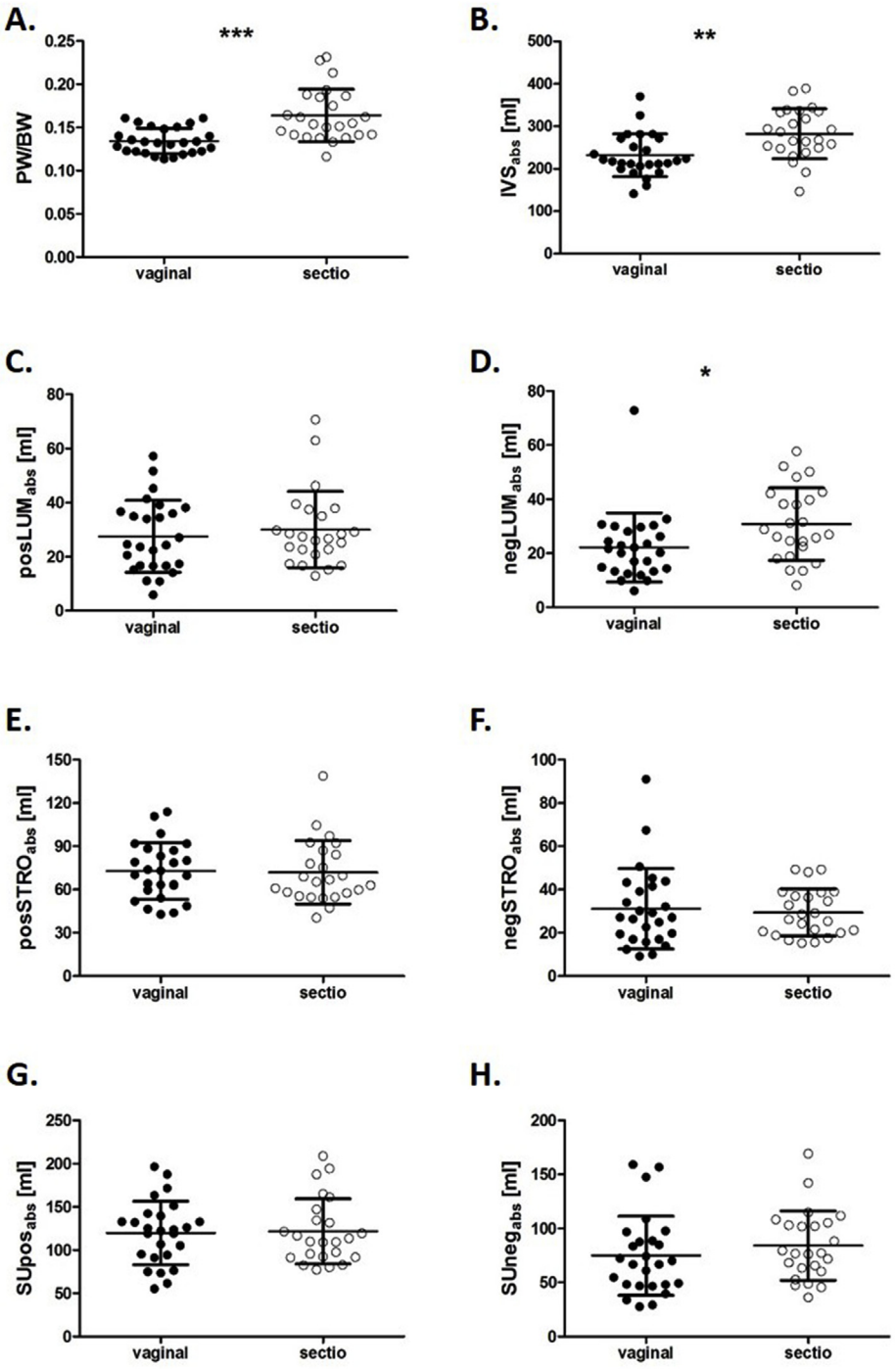

Fig. 5. The boxplots **A.-H.** analyse the influence of delivery mode on parameters of the present study. Data of placentas with vaginal delivery (closed dots) or delivery by cesarean section (open dots) are shown. The tiles show the ratio of placental weight to birth weight (PW/BW; **A.**), the absolute volume of the intervillous space (IVS_{abs}; **B.**), the volume of vessel lumina derived from γ-sm-actin positive villous cross sections ($posLUM_{abs}$; **C.**), the volume of vessel lumina derived from γ-sm-actin negative villous cross sections ($negLUM_{abs}$; **D.**), the volume of stroma derived from γ-sm-actin positive villous cross sections ($posSTRO_{abs}$; **E.**), the volume of stroma derived from γ-sm-actin negative villous cross sections ($negSTRO_{abs}$; **F.**), the sum of all subvolumes derived from γ-sm-actin positive villous cross sections ($SUpos_{abs}$; **G.**), and the sum of all subvolumes derived from γ-sm-actin negative villous cross sections ($SUneg_{abs}$; **H.**). Only the vascular compartments IVS_{abs} (**B.**), $negLUM_{abs}$ (**D.**), and PW (relative to BW, **A.**) are significantly larger/higher than after vaginal delivery as tested for significance by Mann-Whitney *t*-test (*** indicates $p < 0.001$, ** indicates $p < 0.01$ and * denotes $p < 0.05$).

thickness [1,2,25,28–30], there is some functional role to be postulated for those central parts of the villous tree, which harbour γ-sm-actin positive myofibfroblasts [6–10]. This is unexpected since many discussions on prenatal programming in the field are focusing selectively on the peripheral areas of the villous trees [31], where the largest part of the materno-fetal exchange zones is present [27,32]. The data of the present study suggest that full functional understanding of the villous trees as a whole needs novel conceptional understanding of the co-operation between peripheral and central parts of the villous tree.

It seems that more or less volume in the central parts of the villous trees (here mainly reflected in $SUpos_{abs}$ and $posSTRO_{abs}$) is not without an effect on long term pregnancy outcomes. Volume is not more than a kind of proxy - though morphometrically accessible - of the functions of the central part of the villous tree. These functions are much less examined and also less understood than the functional role of the peripheral parts of the villous tree. Data of pathological placentas of preeclampctic pregnancies already point in the direction that the morphology and the internal construction of the stromal part of the central villous trees is different from normal [8,33–35] and thus could be functionally more relevant than actually expected. It is unclear at the moment whether any changes in the perivascular compartment of the central parts of the villous tree could indirectly influence the efficacy of exchange in the peripheral parts of the villous tree. The correlations of the present study were mainly associated with the stromal compartment of the central parts of the villous tree, a region in which the perivascular contractile sheath is in abundance.The present study was not designed to decide on the question whether potential effects of the central villous compartment on overall pregnancy outcome might arise

directly in this position, or might be indirectly transmitted by an influence of the central parts of the villous tree on the efficacy of maternofetal exchange in the peripheral areas of the villous tree.

However, during placental development, the more central parts of the villous tree that harbor perivascular villous myofibroblasts at birth develop earlier as the more peripheral parts of the villous tree [27,32,36]. The staining and analysis method of the present study could thus enable a view back in earlier pregnancy, and could enable indirect and post-hoc access to the mid term adaptive phases of the villous tree, especially in the critical phase of structural remodelling during the 2nd trimester. The second trimester of pregnancy is the time where immature intermediate villi transform and mature to stem villi thereby developing the perivascular contractile sheath [27,32]. It is certainly worth a notion that preeclampsia and intrauterine growth retardation are obstetrical syndromes, which become clinically symptomatic shortly after these maturation steps [27,37].

That the PW/BW ratio and the volumes of the IVS and $negLUM_{abs}$ of fetal capillaries is influenced by the delivery mode (Fig. 5) confirms actual knowledge [38,39]. In contrast to these volumes, which both correspond to important placental blood spaces (IVS and capillary lumen), the stroma volumes of the villous trees (especially $posSTRO_{abs}$, but also $negSTRO_{abs}$) represent structured tissues, the volumes of which are unlikely to substantially depend on obstetric practice. This is also underlined in the present study; we did not find an influence of delivery mode on $posSTRO_{abs}$ and $negSTRO_{abs}$. This qualifies the stromal compartments of the villous tree ($posSTRO_{abs}$ and $negSTRO_{abs}$) as a preserved structural postnatal feature. $posSTRO_{abs}$ and $negSTRO_{abs}$ could serve as novel histodiagnostic targets in future studies on perinatal programming.

In conclusion, the present study shows, for the first time, that volumes belonging to the more centrally located parts of the villous trees reflect weight and thickness of human placentas at microscopic scale.

Authors contributions

AB performed the microscopic analysis. EH and HGF designed the study. FvK was responsible for obstetrical tasks. EH, NB and HGF prepared figures and tables. NB, EH, HGF, CS and FvK wrote the manuscript.

Conflicts of interest

The authors declare no conflict of interest.

Acknowledgements

The authors acknowledge the skillful technical assistance and diligent work of the entire team of technicians of the Department of Anatomy II at LMU Munich, namely B. Aschauer. A. Baltruschat, S. Kerling, B. Mosler and S. Tost. We would also like to express our thanks to the obstetricians, midwives, and nurses of the hospital Dritter Orden (Munich, Germany) who enabled the clinical work of this study with great care and engagement. Funding was provided by the Deutsche Forschungsgemeinschaft (DFG Fr1245/9-1, to HGF).

Appendix A. dSupplementary data

Supplementary data to this article can be found online at https://doi.org/10.1016/j.placenta.2019.08.082.

References

[1] G. Burton, D. Barker, A. Moffett, K. Thornburg (Eds.), The Placenta and Human Developmental Programming, Cambridge University Press, Cambridge, 2011.
[2] G.J. Burton, A.L. Fowden, K.L. Thornburg, Placental origins of chronic disease, Physiol. Rev. 96 (4) (2016) 1509–1565.
[3] P. Kaufmann, D.K. Sen, G. Schweikhart, Classification of human placental villi. I. Histology, Cell Tissue Res. 200 (3) (1979) 409–423.
[4] M.R. Jackson, T.M. Mayhew, P.A. Boyd, Quantitative description of the elaboration and maturation of villi from 10 weeks of gestation to term, Placenta 13 (2015) 357–370.
[5] E. Haeussner, B. Aschauer, G.J. Burton, B. Huppertz, F. Edler von Koch, J. Müller-Starck, C. Salafia, C. Schmitz, H.-G. Frank, Does 2D-Histologic identification of villous types of human placentas at birth enable sensitive and reliable interpretation of 3D structure? Placenta 36 (12) (2015) 1425–1432.
[6] G. Kohnen, S. Kertschanska, R. Demir, P. Kaufmann, Placental villous stroma as a model system for myofibroblast differentiation, Histochem. Cell Biol. 105 (6) (1996) 415–429.
[7] R. Graf, J.U. Langer, G. Schonfelder, T. Oney, S. Hartel-Schenk, W. Reutter, H.H. Schmidt, The extravascular contractile system in the human placenta. Morphological and immunocytochemical investigations, Anat. Embryol. 190 (6) (1994) 541–548.
[8] R. Graf, H. Neudeck, R. Gossrau, K. Vetter, Elastic fibres are an essential component of human placental stem villous stroma and an integrated part of the perivascular contractile sheath, Cell Tissue Res. 283 (1) (1995) 133–141.
[9] R. Demir, G. Kosanke, G. Kohnen, S. Kertschanska, P. Kaufmann, Classification of human placental stem villi: review of structural and functional aspects, Microsc. Res. Tech. 38 (1–2) (1997) 29–41.
[10] R. Spanner, Mütterlicher und kindlicher Kreislauf der menschlichen Placenta und seine Strombahnen, Anat. Embryol. 105 (2) (1935) 163–242.
[11] C. Schmitz, P.R. Hof, Design-based stereology in neuroscience, Neuroscience 130 (4) (2005) 813–831.
[12] T.M. Mayhew, Stereology and the placenta: where's the point? – a review, Placenta 27 (2006) S17–S25.
[13] M. Lahti-Pulkkinen, M.J. Cudmore, E. Haeussner, C. Schmitz, A.-K. Pesonen, E. Hämäläinen, P.M. Villa, S. Mehtälä, E. Kajantie, H. Laivuori, R.M. Reynolds, H.-G. Frank, K. Räikkönen, Placental morphology is associated with maternal depressive symptoms during pregnancy and toddler psychiatric problems, Sci. Rep. 8 (1) (2018) 791.
[14] E. Thomson, Quantitative microscopic analysis, J. Geol. 38 (1930) 193–222.
[15] T.M. Mayhew, C. Sampson, Maternal diabetes mellitus is associated with altered deposition of fibrin-type fibrinoid at the villous surface in term placentae, Placenta 24 (5) (2003) 524–531.
[16] Y. Benjamini, Y. Hochberg, Controlling the false discovery rate: a practical and powerful approach to multiple testing, J. R. Stat. Soc. B 57 (1995) 289–300.
[17] R. Core Team, R.:A. Language, And Environment for Statistical Computing, (2013).
[18] William Revelle, Psych: Procedures for Psychological, Psychometric, and Personality Research, (2018).
[19] John Fox, Sanford Weisberg, An R Companion to Applied Regression, second ed., Sage, Thousand Oaks CA, 2011.
[20] K.H. Ahn, J.H. Lee, G.J. Cho, S.-C. Hong, M.-J. Oh, H.-J. Kim, Placental thickness-to-estimated foetal weight ratios and small-for-gestational-age infants at delivery, J. Obstet. Gynaecol. 37 (7) (2017) 883–887.
[21] C. Vachon-Marceau, S. Demers, S. Markey, N. Okun, M. Girard, J. Kingdom, E. Bujold, First-trimester placental thickness and the risk of preeclampsia or SGA, Placenta 57 (2017) 123–128.
[22] A.J. Lee, M. Bethune, R.J. Hiscock, Placental thickness in the second trimester: a pilot study to determine the normal range, J. Ultrasound Med. 31 (2) (2012) 213–218.
[23] B. Almog, F. Shehata, S. Aljabri, I. Levin, E. Shalom-Paz, A. Shrim, Placenta weight percentile curves for singleton and twins deliveries, Placenta 32 (1) (2011) 58–62.
[24] D.A. Coall, A.K. Charles, C.M. Salafia, Gross placental structure in a low-risk population of singleton, term, first-born infants, Pediatr, Devel. Patho. 12 (3) (2011) 200–210.
[25] D.J.P. Barker, G. Larsen, C. Osmond, K.L. Thornburg, E. Kajantie, J.G. Eriksson, The placental origins of sudden cardiac death, Int. J. Epidemiol. 41 (5) (2012) 1394–1399.
[26] P.R. Nielsen, P.B. Mortensen, C. Dalman, T.B. Henriksen, M.G. Pedersen, C.B. Pedersen, E. Agerbo, Fetal growth and schizophrenia: a nested case-control and case-sibling study, Schizophr. Bull. 39 (6) (2013) 1337–1342.
[27] K. Benirschke, G. Burton, R.N. Beargen, Pathology of the Human Placenta, sixth ed., Springer, Berlin and London, 2012.
[28] D. Barker, K. Thornburg, C. Osmond, E. Kajantie, J. Eriksson, The surface area of the placenta and hypertension in the offspring in later life, Int. J. Dev. Biol. 54 (2–3) (2010) 525–530.
[29] D. Barker, J.G. Eriksson, S.H. Alwasel, C.H.D. Fall, T.J. Roseboom, C. Osmond, The maternal and placental origins of chronic disease, in: G. Burton, D. Barker, A. Moffett, K. Thornburg (Eds.), The Placenta and Human Developmental Programming, Cambridge University Press, Cambridge, 2011, pp. 5–16.
[30] J. Eriksson, E. Kajantie, K. Thornburg, C. Osmond, D. Barker, Mother's body size and placental size predict coronary heart disease in men, Eur. Heart J. 32 (18) (2011) 2297–2303.
[31] G.J. Burton, E. Jauniaux, Development of the human placenta and fetal heart: synergic or independent? Front. Physiol. 9 (2018) 373.
[32] H.-G. Frank, Placental development, in: R.A. Polin, S.H. Abman, D.H. Rowitch, W.E. Benitz, W.W. Fox (Eds.), Fetal and Neonatal Physiology, vol. 1, Elsevier, Philadelphia, 2016, pp. 101–113.
[33] R. Graf, H. Frank, T. Öney, Histochemical and immunocytochemical investigations of the fetal extravascular and vascular contractile system in the normal placenta and during pre-eclampsia, in: D. Neubert, R. Kavlock, H. Merker, J. Klein (Eds.), Risk Assessment of Prenatally-Induced Adverse Health Effects, Springer, Berlin, 1992, pp. 537–550.

[34] D. Wilhelm, U. Mansmann, H. Neudeck, D. Matejevic, K. Vetter, R. Graf, Increase of segments of elastic-type blood vessel walls in fetal placental stem villi during pre-eclampsia at term, Anat. Embryol. 200 (6) (1999) 597–605.
[35] D. Wilhelm, U. Mansmann, H. Neudeck, D. Matejevic, K. Vetter, R. Graf, Decrease of elastic tissue fibres in stem villus blood vessels of the human placenta during IUGR and IUGR with concomitant pre-eclampsia, Anat. Embryol. 205 (5–6) (2002) 393–400.
[36] M. Castellucci, M. Scheper, I. Scheffen, A. Celona, P. Kaufmann, The development of the human placental villous tree, Anat. Embryol. 181 (2) (1990) 117–128.
[37] P. Gathiram, J. Moodley, Preeclampsia: its pathogenesis and pathophysiolgy, Cardiovasc. J. Afr. 27 (2) (2016) 71–78.
[38] S. Porat, B. Fitzgerald, E. Wright, S. Keating, Kingdom, J C P, Placental hyperinflation and the risk of adverse perinatal outcome, Ultrasound Obstet, Gynecology 42 (3) (2013) 315–321.
[39] T.M. Mayhew, F.B. Sorensen, J.G. Klebe, M.R. Jackson, The effects of mode of delivery and sex of newborn on placental morphology in control and diabetic pregnancies, J. Anat. 183 (Pt 3) (1993) 545–552.